



Inhibitory effect of Fingolimod on head and neck squamous cell carcinoma and its mechanism: Gene set enrichment analysis

Lemeng Chang^{1*}, Chunhua Xie¹, Kaiping Chou², Qingnan Meng³, Lihui Zhao⁴

¹ Pharmacy Intravenous Admixture Service, The Second Affiliated Hospital of Qiqihar Medical University, Qiqihar 161006, China

² Department of MRI, The Second Affiliated Hospital of Qiqihar Medical University, Qiqihar 161006, China

³ Department of Rehabilitation Medicine, The Second Affiliated Hospital of Qiqihar Medical University, Qiqihar 161006, China

⁴ Department of Intensive Care Medicine, The Second Affiliated Hospital of Qiqihar Medical University, Qiqihar 161006, China

ARTICLE INFO

Original paper

Article history:

Received: April 25, 2023

Accepted: July 16, 2023

Published: July 31, 2023

Keywords:

Fingolimod, HNSC, GSEA analysis, Cell cycle, PLK1

ABSTRACT

This study aimed to clarify the therapeutic effect of Fingolimod on head and neck squamous cell carcinoma (HNSC) and initially explore its mechanism through data mining, clinical sample analysis and basic experiments. The normalized Enrichment Score (NES) of Fingolimod in tumor tissues was obtained by Swiss-TargetPrediction and The Cancer Genome Atlas (TCGA) database. IC50 (50% inhibitory concentration) of Fingolimod for HNSC was verified based on the Genomics of Drug Sensitivity in Cancer (GDSC) database. SCC9 cells were cultured in vitro for the application of Fingolimod. Cell proliferation was determined by the Cell Counting Kit-8 (CCK-8). The expression levels of genes were determined by reverse transcription-polymerase chain reaction (RT-PCR). The molecular regulatory mechanism of Fingolimod acting on HNSC was analyzed with WebGestalt. Cyclin expression was determined by Western blot assay. The key targeted genes for Fingolimod against HNSC were screened with the TCGA database and verified in clinical samples. Gene Set Enrichment Analysis (GSEA) showed the highest NES score in HNSC (NES=1.53, P<0.05). GDSC showed the lowest IC50 in Fingolimod SCC9 cells. IC50 calculated by the cell activity detected by CCK8 was 4.34 $\mu\text{mol/L}$, and RT-PCR showed significantly suppressed expression of proliferation-related gene Ki-67 after adding Fingolimod (P<0.05). Kyoto Encyclopedia of Genes and Genomes (KEGG) enrichment analysis revealed that the targeted genes for Fingolimod were mainly enriched in cell cycle-related pathways. Western blot showed significantly decreased cyclin expression in SCC9 cells after the treatment with Fingolimod (P<0.05). TCGA analysis revealed that PLK1 is a key targeted gene for Fingolimod in the treatment of HNSC. RT-PCR showed the significantly increased activity of SCC9 after over-expressing PLK1, and the increased proliferation and anti-apoptosis abilities (P<0.05), as well as the significantly inhibited expression of Ki-67 and Bcl-2 after adding Fingolimod. Fingolimod can promote the arrest in G0/G1 of SCC9 cells, and PLK1 is a key targeted gene for the treatment of HNSC. Fingolimod can inhibit cell proliferation caused by PLK1 over-expression.

Doi: <http://dx.doi.org/10.14715/cmb/2023.69.7.24>

Copyright: © 2023 by the C.M.B. Association. All rights reserved.

Introduction

Head and neck squamous cell carcinoma (HNSCC, HNSC), as one of the most common malignancies of the head and neck, accounts for about 90% of head tumors and 16-40% of all tumors in the body (1). The findings of epidemiological investigations show that about 600,000 new cases of HNSC occur annually worldwide. HNSC has the characteristics of increasing morbidity and mortality year by year (2). Therefore, how to achieve effective treatment for HNSC is a hot topic in clinical research. At present, the main clinical treatment for HNSC is surgery combined with chemotherapy (3). However, studies show that the current 5-year overall survival (OS) of HNSC after clinical treatment is about 40-50%. At the same time, due to the anatomical structure specificity of HNSC, surgery for HNSC is also very difficult and risky.(4,5).

Fingolimod, as a sphingosine analog, is currently a representative sphingosine-1-phosphate 1 (S1P1) receptor regulator in clinical practice, which is closely related to

the regulation of the body's immune system (6). Previous studies on Fingolimod were limited to immune system diseases, which are effective in various autoimmune diseases such as relapse-remitting multiple sclerosis (7-9). Recent deep research on Fingolimod has found that Fingolimod also has an effective control effect on tumors (10). It has been shown that Fingolimod can effectively induce apoptosis and inhibit cell proliferation of tumors, thus achieving its anti-tumor effect (11). At present, Fingolimod has been shown in vitro to effectively regulate the disease progression of various tumors such as non-small cell adenocarcinoma and pancreatic cancer (12,13). Nonetheless, there is no research progress on whether Fingolimod has a therapeutic effect on HNSC. In order to investigate the effect of Fingolimod on HNSC, we explored it at the molecular level. With the deepening research on data mining, Gene Set Enrichment Analysis (GSEA) is regarded as a more effective tool in data mining. GSEA detects expression changes in gene sets rather than individual genes, and thus it can contain more comprehensive gene expression

* Corresponding author. Email: changlemeng0202@163.com

changes, and obtain more desired results as expected (14).

Therefore, this study was designed to preliminarily demonstrate the therapeutic potential of Fingolimod on HNSC through data analysis, as well as further verify our results through clinical samples and clarify the mechanism involved by in vitro cellular experiments.

Materials and Methods

Bioinformatics analysis method

Targets for Fingolimod were predicted in the Swiss-TargetPrediction database (<http://www.swisstargetprediction.ch/>), and the information of targets for Fingolimod was screened by setting the species to "homo sapiens" Probability>0.1. RNA sequencing results of the corresponding tumors and the control group were collected from the "The Cancer Genome Atlas" (TCGA) database with a sample size of more than 10. Based on the targets for Fingolimod, the potential effects of Fingolimod in various tumor tissues were obtained by Gene Set Enrichment Analysis (GSEA) and were ranked according to Normalized Enrichment Score (NES). IC50 (50% inhibitory concentration) score of Fingolimod in 987 cell lines of various tumors was obtained through the Genomics of Drug Sensitivity in Cancer (GDSC) database, and the cell lines were compared into two groups according to whether they were an HNSC cell line. All types of cells of HNSC cell lines were extracted and bar charts were drawn to show Fingolimod's IC50 score within various HNSC cell lines. RNA sequencing results from HNSC patients and control patients were downloaded from the TCGA database, and Bayesian analysis was performed with the limma package of R software, to obtain significantly differentially expressed genes of Fingolimod on HNSC. Kaplan-Meier analysis on the survival curves of overall survival (OS) based on the expression levels of differentially expressed genes, to finally identify the key target for Fingolimod on HNSC tumor tissues. Based on the obtained t values of targeted genes for Fingolimod on HNSC, Kyoto Encyclopedia of Genes and Genomes (KEGG) pathway analysis was performed at the WebGestalt website (<http://www.webgestalt.org/>), to clarify the molecular mechanism of Fingolimod regulation of HNSC.

Acquisition of clinical samples

Fifteen cases of HNSC tissues and 15 cases of paracancerous tissues (control group) were selected from the Oncology Department of our hospital from November 2018 to November 2020. The average age of HNSCC patients was 47.89±12.23 years old, including 10 male patients and 5 female patients. All patients none of which received radiotherapy, chemotherapy, immunotherapy and other adjuvant therapies before surgery. All tissue specimens were maintained at -80°C. Patients and their families volunteered to participate in the study and signed the informed consent form. This study was approved by the Medical Ethics Committee of our hospital.

Cell experiments

Source of reagents, antibodies and kits

RPMI-1640 medium (Gibco, Rockville, MD, USA, 31800022), FCS (Hyclone, South Logan, UT, USA, SH30396.03), PBS solution containing double antibodies

(Hyclone, South Logan, UT, USA, SH30256.01), CCK-8 kit (Solabio Technology, Beijing, China, CA1210), reverse transcription kit (TaKaRa, Tokyo, Japan, RR047A), qPCR kit (TaKaRa, Tokyo, Japan, RR430B). PLK1-ov and PLK1-ov-control lentiviruses were constructed, sequenced, produced, titer determined, packaged, transported and cold-chain delivered to the laboratory by Shanghai Genechem Co., LTD. (Shanghai, China).

Cell culture

SCC9 (human tongue squamous cell carcinoma cell line) (CRL-1629) was purchased from American Type Culture Collection (ATCC) (Manassas, VA, USA, Cat. No.: JH-H1639). SCC9 cells were cultured in PRMI 1640 medium containing 10% FBS and 1% double antibodies. Cellular carcinoma was cultured in a constant-temperature incubator at 37°C, with 5% CO₂. The fluid of cells was replaced every day, with the observation of the cell density under an inverted microscope. When the cell density reached 80%, the cells were sub-cultured.

The Cell Counting Kit-8 (CCK-8) experiment

CCK-8 assessment for the effect of Fingolimod at different concentrations on the activity of SCC9 cells

Cells were divided into 0, 5, 10, 15, 20, and 25 µmol/L groups, and Fingolimod solution at a corresponding concentration was added to each group. After being treated under different treatment conditions to different groups, SCC9 was inoculated in 96-well plates, and then incubated in the constant-temperature incubator, and cell proliferation capacity was detected by CCK-8 at 0, 24 h and 72 h after inoculation. The procedures were: remove 96-well plates from the constant-temperature incubator, absorb the medium in each well and add 100ul of CCK8 solution to each well, and then place in the constant-temperature incubator for 2 h, and finally determine the OD of each well at a wavelength of 450 nm.

CCK-8 assessment for the effect of Fingolimod and PLK1 on SCC9 cell activity

Cells were divided into control, PLK1-ov, PLK1-ov-control, and PLK1-ov + Fingolimod groups. After being treated under different treatment conditions to different groups, SCC9 was inoculated in 96-well plates, and then incubated in the constant-temperature incubator, and cell proliferation capacity was detected by CCK-8 at 0, 24 h and 72 h after inoculation. The procedures were: remove 96-well plates from the constant-temperature incubator, absorb the medium in each well and add 100 ul of CCK8 solution to each well, and then place in the constant-temperature incubator for 2 h, and finally determine the OD of each well at a wavelength of 450 nm.

Lentivirus infection

Transfections with PLK1-ov, PLK1-ov-control and PLK1-ov-control lentivirus were performed for PLK1-ov, PLK1-ov-control and PLK1-ov + Fingolimod group, respectively. SCC9 cell lines were taken as the research object, and the cells were tryptically digested and re-suspended after the growth density of cells reached 80%. The obtained cells were inoculated at 1×10⁵/well in 6-well plates and incubated in the constant-temperature incubator at 37°C for 24 h to the adherent state. The purchased

PLK1-ov-control and PLK1-ov-control lentiviruses were diluted with the PRMI 1640 solution containing 10% FBS at the ratio of 1:10 according to different groups of cells. After discarding the medium in 6-well plates, 1ml of dilution containing lentivirus was added to each well, which was incubated in the constant-temperature incubator at 37°C for 24 h, and then the medium containing lentivirus was discarded. 2ml of PRMI 1640 medium containing 10% FBS was added, which was incubated in the constant-temperature incubator.

Quantitative real time polymerase chain reaction (qRT-PCR)

SCC9 cells in the logarithmic growth phase were inoculated in 6-well plates and incubated in the incubator after adding PLK1-ov-control lentivirus, PLK1-ov-control lentivirus, PLK1-ov-control lentivirus and Fingolimod for 72 h, respectively. Cells of each group were collected, and tissue/cell contents were obtained with the cell lysate. Total RNA in the cells was extracted by the TRIzol assay and the concentration and purity of RNA in the solution were determined. A reverse transcription reaction system was established with the Takara reverse transcription kit, which reversed RNA into cDNA, and a cDNA reaction system was established with a qPCR kit by qRT-PCR amplification. The PCR reaction system is 10 μ L of TB Green Premix Ex Taq II and 0.4 μ L of ROX Reference Dye II, with 0.8L for each of upstream and downstream primers, 6 μ L of ddH₂O and 2 μ L of cDNA. The sequences of PCR primers are shown in Table 1. PCR reaction conditions were: 95°C for 10 min, 95°C for 30 s, 60°C for 30 s, for 40 cycles in total. The final data were analyzed statistically by $2^{-\Delta\Delta CT}$ for related gene expression levels in each sample.

Western blot

SCC9 cells in the logarithmic growth phase were inoculated in 6-well plates and incubated in the incubator after adding PLK1-ov-control lentivirus, PLK1-ov-control

Table 1. PCR primer construction.

Gene	Primers
Ki -67	F 5'CGCCTGGTTACTATCAAAAG3' R 5'CAGACCCATTTACTTGTGTTGG3'
Bcl-2	F 5' GCTACTGCTGATGCTGTC3' R 5' TGTGCCTATTACCTACTATGC3'
PLK1	F 5'CAGTCACTCTCCGCGACAC3' R 5'GAGTAGCCGAATTGCTGCTG3'
β -actin	F 5'ACATCCGTAAAGACCTCTATGCC3' R 5'TACTCCTGCTTGCTGATCCAC3'

Table 2. Specific information on antibodies and reagents.

Antibody	Company	Art. No.	Concentration
CyclinD1	abcam, UK	ab16663	1:1000
CDK4	abcam, UK	ab108357	1:1000
CDK6	abcam, UK	ab124821	1:5000
p-CDK4	abcam, UK	ab277788	1:1000
p-CDK6	Thermo Fisher, USA	PA5-118525	1:1000
Goat Anti-Mouse IgG	Bioss, Beijing	bs-0296G	1:3000
Goat Anti-rabbit IgG	Bioss, Beijing	bs-0295G	1:3000
GAPDH	Santa Cruz, USA	sc-47724	1:1000

lentivirus, PLK1-ov-control lentivirus and Fingolimod for 72 h, respectively. Cells of each group were collected, and tissue/cell contents were obtained with the cell lysate. Total cell proteins were collected by centrifugation. Protein concentration was detected quantitatively according to the bicinchoninic acid (BCA) assay. After that, an appropriate amount of proteins from each group was collected for 12% sodium dodecyl sulphate-polyacrylamide gel electrophoresis (SDS-PAGE) electrophoresis to separate proteins, with the conditions of 80 V for 30 min and 120 V for 70 min. After the electrophoresis, the proteins separated by electrophoresis were transferred to a polyvinylidene fluoride (PVDF) membrane with a transfer device, and the transfer time was appropriately adjusted according to the size of the relative molecular mass of proteins. PVDF membrane was removed after the membrane transferring and blocked with 5% skim milk for 1 h. The primary antibody was subsequently incubated at 4°C overnight, and was washed 3 times the next day with 1×PBST for 10 min each. HRP-labeled sheep anti-rabbit antibody was then added as the secondary antibody for 1 h. Finally, the PVDF membrane was exposed to a chemiluminescence imaging system for detection. The grayscale value of the protein bands was analyzed with Image J software, with the ratio of the grayscale value of the target protein to internal reference glyceraldehyde 3-phosphate dehydrogenase (GAPDH) protein band as the relative expression of the target protein. The specific information of antibodies is detailed in Table 2.

Statistical analysis

The statistical analysis of this study was performed by R 4.1.0 and Statistical Product and Service Solutions (SPSS) 26.0 software (IBM, Armonk, NY, USA). Bayesian analysis was performed with the limmar package of R software for data mining, $P < 0.05$, $|\log_2 FC| \geq 1$ was taken as the differential gene screening criteria. Corresponding statistical analysis was performed with SPSS26.0 for clinical studies and basic experimental studies. The obtained data were expressed as mean \pm standard deviation (SD), the comparisons between multiple groups were analyzed by ANOVA, and the indexes with statistically significant ANOVA results were subjected to the Turkey HSD post-hoc test, respectively. $P < 0.05$ was considered as statistically significant.

Results

GSEA analysis clarified the potential role of Fingolimod in HNSC

In this study, the targeted genes for Fingolimod were

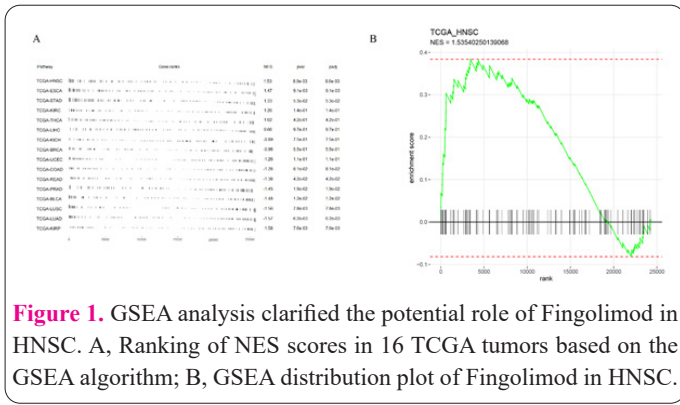


Figure 1. GSEA analysis clarified the potential role of Fingolimod in HNSC. A, Ranking of NES scores in 16 TCGA tumors based on the GSEA algorithm; B, GSEA distribution plot of Fingolimod in HNSC.

analyzed through the Swiss Target Prediction website, and its set files were obtained. Genome-wide RNAseq data from 16 tumors (controls were greater than or equal to 10) were downloaded from the TCGA database. Genome-wide rank was obtained by Bayesian analysis of R software, and NES scores of 16 tumors were obtained through GSEA analysis (Figure 1A, B and Supplementary Figure 1). According to the sequencing results, the NES score of Fingolimod in HNSC was significantly higher than that in the other 15 tumors, and the difference was statistically significant ($NES=1.53, P=8.0 \times 10^{-3}$). Therefore, this study considers that Fingolimod has a high application value in HNSC.

Fingolimod inhibited cell proliferation in HNSC

In this study, Fingolimod's IC50 scores in 987 cell lines of various tumors were obtained through the Genomics of Drug Sensitivity in Cancer (GDSC) database, comparing IC50 scores in cancer cell lines of head and neck squamous cell lines with other tumor cell lines. The results showed that Fingolimod had significantly lower IC50 in HNSC

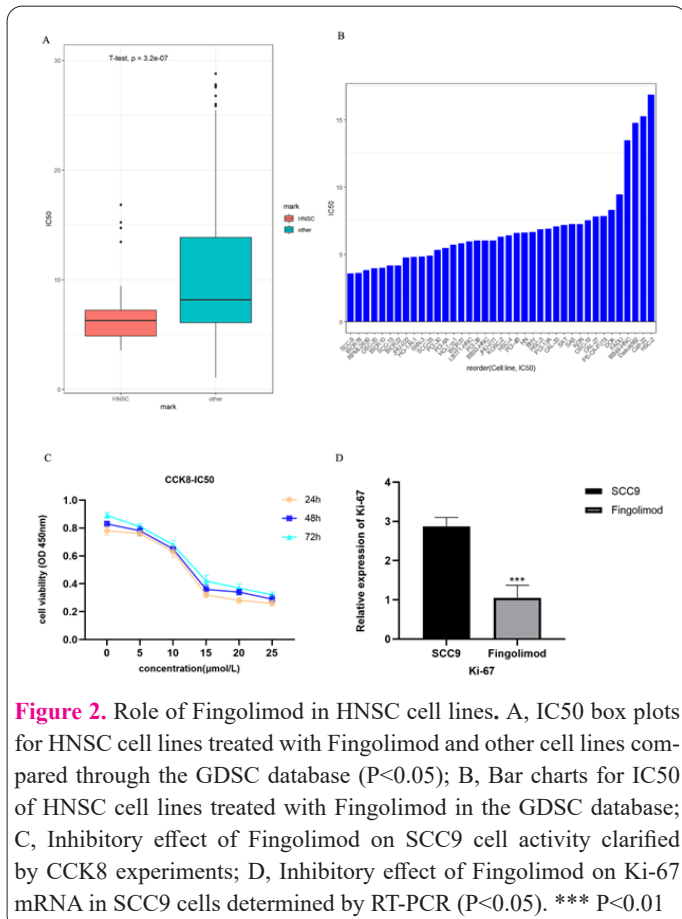


Figure 2. Role of Fingolimod in HNSC cell lines. A, IC50 box plots for HNSC cell lines treated with Fingolimod and other cell lines compared through the GDSC database ($P<0.05$); B, Bar charts for IC50 of HNSC cell lines treated with Fingolimod in the GDSC database; C, Inhibitory effect of Fingolimod on SCC9 cell activity clarified by CCK8 experiments; D, Inhibitory effect of Fingolimod on Ki-67 mRNA in SCC9 cells determined by RT-PCR ($P<0.05$). *** $P<0.01$

than that in other tumor cell lines (Figure 2A). Bar charts for the IC50 score of Fingolimod within each cell line of HNSC showed Fingolimod's lowest IC50 score in SCC9 (Figure 2B). Taking the SCC9 cell line as the research object, CCK8 results showed that the inhibition of Fingolimod on cell activity increased with increasing dose, calculating an IC50 as $4.34 \mu\text{mol/L}$ (Figure 2C). After co-culturing SCC9 cells with Fingolimod at a concentration of $5 \mu\text{mol/L}$, RT-PCR showed significantly decreased expression of the cell proliferation-associated gene Ki-67 (Figure 2D). The results of this part showed that the inhibitory effect of Fingolimod was significantly higher on the proliferation of HNSC cell lines than that of other tumor cell lines, and was the most significant on the proliferation of SCC9 cells in HNSC cell lines.

Fingolimod regulated the arrest in G0/G1 of SCC9 cells

KEGG pathway analysis on the targeted genes for Fingolimod based on the WebGestalt website showed a correlation with the cell cycle pathway (Figure 3A, $FDR \leq 0.05$). To elucidate the molecular mechanism of Fingolimod in the proliferation of HNSC, the cell cycle distribution of HNSC was examined by flow cytometry. Western blot assay revealed the expression of proteins controlling the cell cycle progression in G0/G1. The results showed that the treatment with Fingolimod at $5 \mu\text{mol/L}$ decreased the expression of CyclinD1, CDK4 and CDK6, and increased the expression of p-CDK4 and p-CDK6 (Figure 3B-G, $P<0.05$). The above results show that Fingolimod achieves the arresting effect on the G0/G1 of SCC9 cells

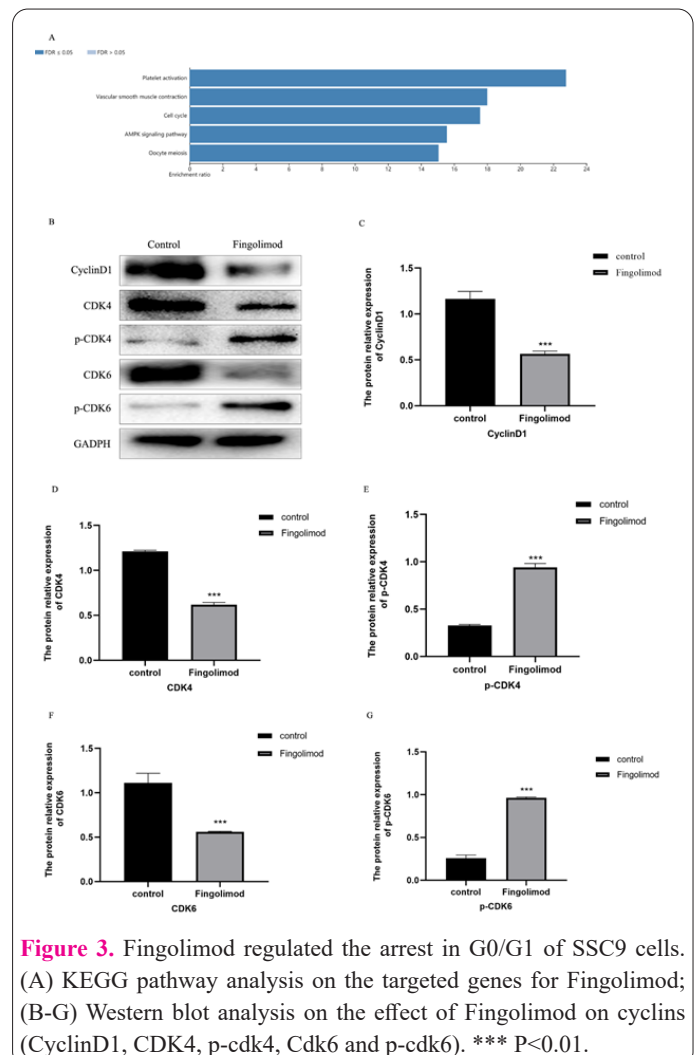


Figure 3. Fingolimod regulated the arrest in G0/G1 of SCC9 cells. (A) KEGG pathway analysis on the targeted genes for Fingolimod; (B-G) Western blot analysis on the effect of Fingolimod on cyclins (CyclinD1, CDK4, p-cdk4, Cdk6 and p-cdk6). *** $P<0.01$.

mainly by promoting the expression and phosphorylation of cyclins.

PLK1 is a key target of Fingolimod for the treatment of HNSC

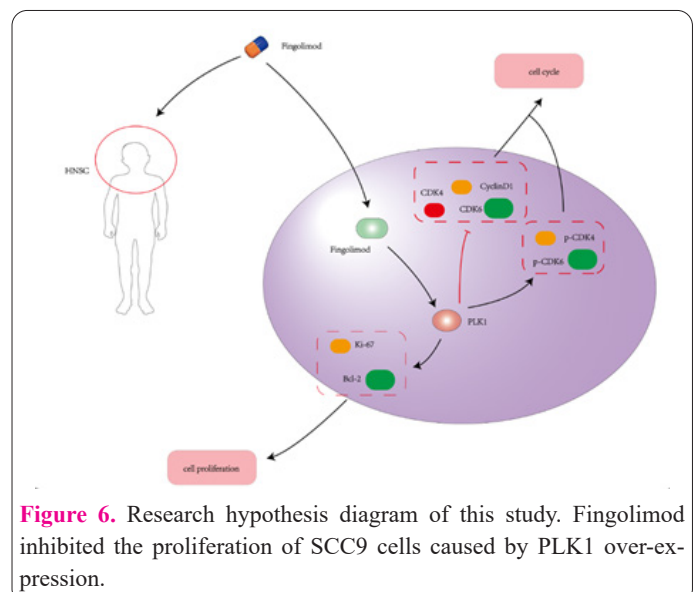
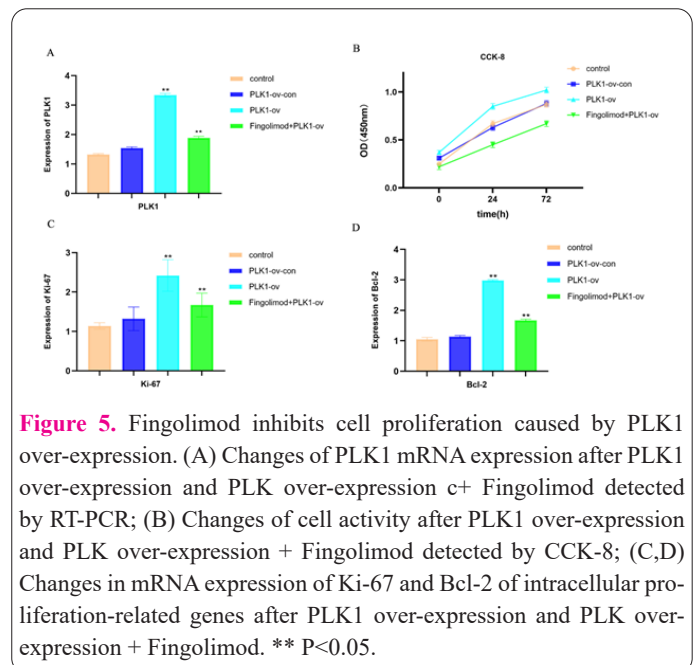
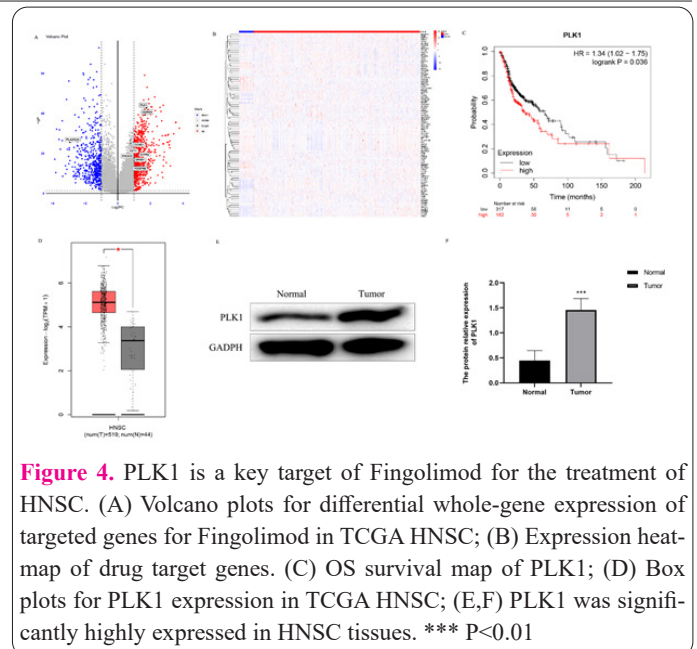
The data of mRNA expression of 502 cases of HNSC and 44 controls were downloaded from the TCGA database. Bayesian analysis was performed with the limmar package of R software, and the results were presented with volcano plots (with the abscissa as \log_2FC , the ordinate as $-\log_{10}(P)$, and the cut-off value of $P < 0.05$, $|\log_2FC| \geq 1$) and marked with significantly expressed targeted genes for Fingolimod (Figure 4A). A heat map was drawn based on the significantly expressed fingolimod target genes, and the results showed that the target genes were differentially expressed in paracancerous tissues and tumor tissues (Figure 4B) and 10 significantly expressed targeted genes were obtained for subsequent analysis. Kaplan-Meier survival analysis was performed based on 10 significantly expressed targeted genes, obtaining OS survival map of each targeted gene (Figure 4C and Supplementary Figure 2), which finally showed the highest significance of PLK1, and PLK1 was identified as the key targeted gene for Fingolimod (logrank $P = 0.036$, $HR = 1.34$). Box plots were drawn to show the expression of PLK1 in TCGA HNSC, which showed that the expression of PLK1 in HNSC was significantly higher than that in the control group (Figure 4D, $P < 0.05$). Clinical samples also revealed a significantly high expression OF PLK1 IN HNSC tissues (Figure 4E, F).

Fingolimod inhibited cell proliferation caused by PLK1 over-expression

To clarify the status of cell proliferation caused by PLK1 over-expression, Fingolimod was added after over-expressing PLK1 of SCC9 cell lines by the lentiviral infection technique. RT-PCR showed a significant up-regulation of PLK1 expression in SCC9 after over-expressing PLK1, and a significant decrease of PLK1 expression after adding Fingolimod (Figure 5A, $P < 0.05$); CCK-8 results showed a significantly increased activity of SCC9 cells after over-expressing PLK1, and a significantly inhibited cellular activity after adding Fingolimod (Figure 5B, $P < 0.05$). The expression of the proliferation-related genes, Ki-67 and Bcl-2, as detected by RT-PCR showed a significantly increased expression of Ki-67 and Bcl-27 after over-expressing PLK1, which was significantly inhibited after adding Fingolimod (Figure 5C,D, $P < 0.05$).

Discussion

In this study, GSEA analysis initially clarified that Fingolimod mainly regulated the cell cycle of HNSC. Western blot showed that Fingolimod could decrease the expression of CyclinD1, CDK4 and CDK6 and increase the expression of p-CDK4 and p-CDK6. Bayes analysis and K-M survival analysis indicated that PLK1 is the key targeted gene for Fingolimod for the treatment for HNSC, in which PLK1 in SCC9 cells was over-expressed by lentivirus infection technique with the application of Fingolimod. The changes in cell activity were detected by CCK-8 and the expression of genes related to cell proliferation was detected by RT-PCR, which clearly showed that Fingolimod can inhibit the proliferation of SCC9 cells caused by



PLK1 over-expression, and its specific regulatory molecular mechanisms can be seen in Figure 6.

Studies have shown that over 60% of patients with

HNSC were advanced at diagnosis, while follow-up after standardized treatment for locally advanced HNSC patients showed a very low 5-year survival of only 40% of them (3). Therefore, developing new effective drugs for HNSC is a hotspot of clinical research. As a sphingosine-1-phosphate receptor modulator, Fingolimod can bind to the S1P1 receptor on the lymphocyte surface after entering the body by phosphorylation, so as to effectively prevent the outflow of newborn lymphocytes from lymph nodes, promote the homing effect of lymphocytes on the eve, and finally realize the regulation of the body's immune system. At present, Fingolimod has been widely used in immune system diseases as well as in the field of tumors. Previous studies have shown that Fingolimod has a good therapeutic effect for autoimmune diseases such as encephalomyelitis and herpes zoster, as well as various tumor animal models such as non-small cell lung cancer and breast cancer (10-14). Fingolimod can achieve an effect on the proliferation and apoptosis of gastric cancer cells by regulating COL11AQ expression (12). Meanwhile, it was shown that Fingolimod can inhibit the malignant proliferation of subcutaneous graft tumors in renal cancer mice by inhibiting P13K/AKT signaling pathways while inducing apoptosis of renal cell carcinoma cells (13). However, the specific effect of Fingolimod on HNSC and its regulatory mechanism for HNSC have not been reported. In this study, SCC9 cells of HNSC were cultured in vitro and added with Fingolimod, showing that SCC9 cell activity was significantly inhibited after adding Fingolimod, and mRNA expression of the proliferation-related gene Ki-67 was also significantly inhibited according to RT-PCR. On this basis, this study suggested that Fingolimod has some inhibitory effect on SCC9 cells.

To further explore the application effect of Fingolimod on HNSC and its mechanism, this study was conducted through data mining and cell validation. The Swiss Target Prediction website was primarily used for initially defining the specific targeted molecular mechanism by which small molecule substances play a pharmacological role (15,16). Meanwhile, GDSC has been widely used to predict the effect of a specific drug on tumors, as well as the concentration of action (17). As a cancer research project established by NCI and NHGRI cosurgery, TCGA database can be used to screen for differentially expressed genes in multiple malignant tissues and matched normal tissue samples, and thus play a great role in the diagnosis, treatment and prevention of tumors. Based on many of the above previous studies, the research team holds that the therapeutic effect of Fingolimod on HNSC and its mechanism can be preliminarily evaluated through data mining. Targeted genes of Fingolimod were obtained from the Swiss website while the differential genes for HNSC were obtained from the TCGA database. GSEA analysis preliminarily clarified that Fingolimod has the highest NES score for HNSC, indicating that Fingolimod has a good application effect for HNSC. Analysis of the GDSC database showed that Fingolimod had significantly lower IC50 for HNSC cell lines than for other cell lines, while analysis of all HNSC cell lines showed that Fingolimod had the lowest IC50 score in SCC9 cell lines. The above data mining results preliminarily clarify that Fingolimod has a good prospect in inhibiting HNSC activity.

To clarify the specific molecular mechanism of Fingolimod acting on HNSC, this study initially showed that

KEGG enrichment analysis for HNSC targeted genes was mainly enriched in cell cycle-related pathways. It has shown that the occurrence and development of most malignancies have the characteristic of cell cycle hyperactivation (18). Effective inhibition of cell cycle activation is a hot topic in the study of tumor diseases. However, this study examined cell cycle changes by flow cytometry, which showed that the proportion of G1/G0 cells and S cells decreased after adding Fingolimod in SCC9. KEGG analysis can effectively promote G1/G0 arrest in SCC9 cells. CyclinD1 acts as an important regulator of cell cycle, showing a significant increase in CyclinD1 expression within breast cancer tumors, thus causing the increased activity of CDK4/6, triggering the activation of downstream genes, and ultimately aggravating the abnormal proliferation in cells (19-21). On this basis, various researchers tried to achieve effective treatment for tumors by inhibiting the activity of CDK4/6. However, the application of CDK4/6 inhibitor to tumor tissues showed a significantly decreased proliferative activity in breast cancer and a significantly increased cellular senescence and apoptosis. Meanwhile, CDK4/6 inhibitor has a good application effect in acute T lymphocytic leukemia, melanoma and non-small-cell lung cancer (22-24). On this basis, Western blot assay verified the significantly inhibited expression of CyclinD1, CDK4 and CDK6 and the increased expression of p-CDK4 and p-CDK6 after adding Fingolimod in this study. Therefore, this study suggested that Fingolimod can exert its therapeutic effect by inhibiting CyclinD1 and promoting the activation of CDK4 and CDK6, thus promoting G0/G1 arrest in SCC9 cells.

To further clarify the key targeted gene for Fingolimod in the treatment of HNSC, this study initially clarified PLK1 as a key targeted gene for Fingolimod in the treatment of HNSC by Bayesian analysis and K-M analysis. As a class of highly conserved silk/threonine protein kinases in structure and functions, PLK1 can be involved in the regulation of different stages of the cell cycle (25). The study on the structure and functions of PLK1 revealed that PLK1 mainly regulates cyclins that act on cells during the G2/M phase. Mucins can be removed from the single arm of chromosomes during mitosis, thus affecting spindle formation and cytoplasmic division (26). The over-expression of PLK1 can cause the formation of various tumors, such as breast cancer, pancreatic cancer, head and neck cancer and non-small-cell lung cancer. Meanwhile, the study showed that PLK1 has become a new target of anti-tumor therapy (27). Researchers have tried to inhibit the PLK1 domain by building inhibitors of the cell cycle (28). For example, some researchers attempt to achieve tumor treatment by designing inhibitors of the ATP domain in PLK1, and relevant studies have been applied in clinical research (29). By applying the PLK1 inhibitor in pediatric patients with acute myeloid leukemia, the researchers showed that tumor cell proliferation was significantly inhibited and apoptosis levels increased (30). Meanwhile, there are many in vitro studies showing that inhibiting PLK1 can effectively inhibit the proliferation capacity of tumor cells as well as cellular activity (31,32). In this study, PLK1 of the SCC9 cell line was over-expressed by the lentivirus infection technique, CCK-8 showed significantly increased cell activity, and RT-PCR showed significantly increased expression of the proliferation-related gene Ki-67. After adding Fingolimod on the basis of

over-expression of PLK1, CCK-8 showed significantly decreased cell activity, and RT-PCR showed significantly decreased expression of proliferation-related genes, Ki-67 and Bcl-2. On this basis, this study suggests that PLK1 is a key target gene for Fingolimod in the treatment of HNSC. Meanwhile, PLK1 can inhibit cell proliferation caused by PLK1 over-expression.

Based on data mining and cell experiments, this study clearly indicates that Fingolimod can achieve G0/G1 arrest in SCC9 cell lines by inhibiting PLK1 expression, to provide a theoretical basis for the clinically effective treatment for HNSC. However, this study is a cell experiment, and the environment of cells cannot effectively simulate the tumor environment in vivo, which has certain limitations.

Fingolimod can exert its therapeutic effect on HNSC by promoting G0/G1 arrest of HNSC cells. PLK1 is a key targeted gene for Fingolimod in the treatment of HNSC. Fingolimod can inhibit cell proliferation caused by PLK1 over-expression.

However, there are still some deficiencies in this paper: first, this study only confirmed that fingolimod regulates cell cycle and cell activity through PLK1, and did not study the characteristics of tumor proliferation and migration; secondly, this study was an in vitro experimental study. In vivo, experimental validation is lacking. The above deficiencies will be verified in the follow-up research.

Funding

This study is funded by the Joint Guidance Project of Qiqihar City Science and Technology Plan (LHYD-202048).

Author contribution

Lemeng Chang and Chunhua Xie conceived and designed the study, and drafted the manuscript. Lemeng Chang, Kaiping Chou, Qingnan Meng and Lihui Zhao collected, analyzed and interpreted the experimental data. Chunhua Xie and Qingnan Meng revised the manuscript for important intellectual content. All authors read and approved the final manuscript.

Conflicts of Interest

The authors have no conflicts of interest to declare.

Ethical approval

The study was approved by the Ethical Committee of The Second Affiliated Hospital of Qiqihar Medical College and conducted in accordance with ethical standards.

References

- de Ruiter EJ, Mulder FJ, Koomen BM, et al. Comparison of three PD-L1 immunohistochemical assays in head and neck squamous cell carcinoma (HNSCC). *Modern Pathol* 2021; 34(6): 1125-1132.
- Chamorro PC, Garcia GA, Padin IE, Rivas MB, Lorenzo PA, Perez SM. Identification of Prognosis Associated microRNAs in HNSCC Subtypes Based on TCGA Dataset. *Medicina-Lithuania* 2020; 56(10): 535.
- Lu S, Sun Z, Tang L, Chen L. LINC00355 Promotes Tumor Progression in HNSCC by Hindering MicroRNA-195-Mediated Suppression of HOXA10 Expression. *Mol Ther-Nucl Acids* 2020; 19: 61-71.
- Li M, Li X, Zhang Y, et al. Micropeptide MIAC Inhibits HNSCC Progression by Interacting with Aquaporin 2. *J Am Chem Soc* 2020; 142(14): 6708-6716.
- Chatfield-Reed K, Gui S, O'Neill WQ, Teknos TN, Pan Q. HPV33+ HNSCC is associated with poor prognosis and has unique genomic and immunologic landscapes. *Oral Oncol* 2020; 100: 104488.
- Hasan AO, Berner F, Ackermann CJ, et al. Fingolimod and tumor-infiltrating lymphocytes in checkpoint-inhibitor treated cancer patients. *Cancer Immunol Immun* 2021; 70(2): 563-568.
- Alping P, Askling J, Burman J, et al. Cancer Risk for Fingolimod, Natalizumab, and Rituximab in Multiple Sclerosis Patients. *Ann Neurol* 2020; 87(5): 688-699.
- Allam RM, Al-Abd AM, Khedr A, et al. Fingolimod interrupts the cross talk between estrogen metabolism and sphingolipid metabolism within prostate cancer cells. *Toxicol Lett* 2018; 291: 77-85.
- White C, Alshaker H, Cooper C, Winkler M, Pchejetski D. The emerging role of FTY720 (Fingolimod) in cancer treatment. *Oncotarget* 2016; 7(17): 23106-23127.
- Booth L, Roberts JL, Spiegel S, Poklepovic A, Dent P. Fingolimod augments Pemetrexed killing of non-small cell lung cancer and overcomes resistance to ERBB inhibition. *Cancer Biol Ther* 2019; 20(5): 597-607.
- Kalhari V, Magnusson M, Asghar MY, Pulli I, Tornquist K. FTY720 (Fingolimod) attenuates basal and sphingosine-1-phosphate-evoked thyroid cancer cell invasion. *Endocr-Relat Cancer* 2016; 23(5): 457-468.
- Canzler S, Hackermuller J. multiGSEA: a GSEA-based pathway enrichment analysis for multi-omics data. *Bmc Bioinformatics* 2020; 21(1): 561.
- Hsu JB, Lee GA, Chang TH, et al. Radiomic Immunophenotyping of GSEA-Assessed Immunophenotypes of Glioblastoma and Its Implications for Prognosis: A Feasibility Study. *Cancers* 2020; 12(10): 3039.
- Takashima Y, Hamano M, Fukai J, et al. GSEA-assisted gene signatures valid for combinations of prognostic markers in PCNSL. *Sci Rep-Uk* 2020; 10(1): 8435.
- Opreescu SN, Horzmann KA, Yue F, Freeman JL, Kuang S. Microarray, IPA and GSEA Analysis in Mice Models. *Bio-Protocol* 2018; 8(17): e2999.
- Elsayed I, Wang X. PLK1 inhibition in cancer therapy: potentials and challenges. *Future Med Chem* 2019; 11(12): 1383-1386.
- Rupp T, Pelouin O, Genest L, Legrand C, Froget G, Castagne V. Therapeutic potential of Fingolimod in triple negative breast cancer preclinical models. *Transl Oncol* 2021; 14(1): 100926.
- Goel S, DeCristo MJ, McAllister SS, Zhao JJ. CDK4/6 Inhibition in Cancer: Beyond Cell Cycle Arrest. *Trends Cell Biol* 2018; 28(11): 911-925.
- Wenzel ES, Singh A. Cell-cycle Checkpoints and Aneuploidy on the Path to Cancer. *In Vivo* 2018; 32(1): 1-5.
- Williams GH, Stoeber K. The cell cycle and cancer. *J Pathol* 2012; 226(2): 352-364.
- Li J, Stanger BZ. Cell Cycle Regulation Meets Tumor Immunosuppression. *Trends Immunol* 2020; 41(10): 859-863.
- Rizk-Rabin M, Chaoui-Ibadioune S, Vaczlavik A, et al. Link between steroidogenesis, the cell cycle, and PKA in adrenocortical tumor cells. *Mol Cell Endocrinol* 2020; 500: 110636.
- Brockelmann PJ, de Jong M, Jachimowicz RD. Targeting DNA Repair, Cell Cycle, and Tumor Microenvironment in B Cell Lymphoma. *Cells-Basel* 2020; 9(10): 2287.
- Naqvi AZ, Mahjabeen I, Ameen S, et al. Genetic and expression variations of cell cycle pathway genes in brain tumor patients. *Bioscience Rep* 2020; 40(5): BSR20190629.
- Montaudon E, Nikitorowicz-Buniak J, Sourd L, et al. PLK1 inhibition exhibits strong anti-tumoral activity in CCND1-driven breast cancer metastases with acquired palbociclib resistance. *Nat*

- Commun 2020; 11(1): 4053.
26. Shin SB, Woo SU, Yim H. Cotargeting Plk1 and androgen receptor enhances the therapeutic sensitivity of paclitaxel-resistant prostate cancer. *Ther Adv Med Oncol* 2019; 11: 432505881.
 27. Reda M, Ngamcherdtrakul W, Gu S, et al. PLK1 and EGFR targeted nanoparticle as a radiation sensitizer for non-small cell lung cancer. *Cancer Lett* 2019; 467: 9-18.
 28. Chen Z, Chai Y, Zhao T, et al. Effect of PLK1 inhibition on cisplatin-resistant gastric cancer cells. *J Cell Physiol* 2019; 234(5): 5904-5914.
 29. Huang WJ, Wang Y, Liu S, et al. Retraction notice to "Silencing circular RNA hsa_circ_0000977 suppresses pancreatic ductal adenocarcinoma progression by stimulating miR-874-3p and inhibiting PLK1 expression" [Cancer Letters 422C (2018) 70-80]. *Cancer Lett* 2018; 438: 232.
 30. Song R, Hou G, Yang J, et al. Effects of PLK1 on proliferation, invasion and metastasis of gastric cancer cells through epithelial-mesenchymal transition. *Oncol Lett* 2018; 16(5): 5739-5744.
 31. Liu Z, Sun Q, Wang X. PLK1, A Potential Target for Cancer Therapy. *Transl Oncol* 2017; 10(1): 22-32.
 32. Gutteridge RE, Ndiaye MA, Liu X, Ahmad N. Plk1 Inhibitors in Cancer Therapy: From Laboratory to Clinics. *Mol Cancer Ther* 2016; 15(7): 1427-1435.